LARGE-SCALE SPARSE RECONSTRUCTION THROUGH PARTITIONED COMPRESSIVE SENSING

Si Qin, Yimin D. Zhang, Qisong Wu, and Moeness G. Amin

Center for Advanced Communications, Villanova University, Villanova, PA 19085, USA

ABSTRACT

Compressive sensing (CS) finds broad applications in various sparse reconstruction problems. It has been clearly established that CS techniques achieve improved quality and resolution for many radar imaging problems where the scene is sparse or can be sparsely represented. One of the major issues that limits the applicability of CS techniques in radar systems is the prohibitive complexity in large-scale imaging problems encountered in, for example, synthetic aperture radar. However, as the actual scene and the back-projection images are associated with the point spreading function which has a finite support, it becomes possible to reconstruct the sparse scene based only on local observations. In this paper, we develop a novel segmented CS technique that achieves nearly optimal sparse reconstruction performance with significant reduction of computation complexity and memory requirements. The effect of interference from neighboring segments is examined, and the conditions of interference-free reconstruction of segmented compressive sensing are devised. The effectiveness of the proposed technique is verified by simulation results.

Index Terms— Compressive sensing, radar imaging, synthetic aperture radar, large-scale scene, back-projection

1. INTRODUCTION

Conventional radar imaging uses Fourier-based methods such as the back-projection algorithm [1, 2, 3]. These algorithms work well when the data are sampled at the Nyquist rate. In practice, we encounter many applications where the observed data are incomplete or undersampled. One of such scenarios is the multistatic passive radar that yields observations in multiple disconnected regions in the wavenumber domain due to multiple narrowband signals corresponding to available illuminators of opportunity [4, 5, 6]. In this case, Fourier-based techniques yield images with a low resolution and high sidelobes. An effective approach to achieve high-resolution images in such scenarios is to use the recent advances of sparse reconstruction and compressive sensing (CS) approaches [7]. Sparse reconstruction methods can accurately reconstruct sparse scenes with a small number of randomly sampled Fourier samples, and can resolve closely spaced targets beyond the Fourier resolution [8, 9].

An important issue to be considered in CS-based radar imaging is the computation and storage requirements determined by the size of the sensing dictionary matrix. This problem is less significant when dealing with small-scale scenes, such as those emerging in ground-based through-the-wall radar imaging (TWRI) and inverse synthetic aperture radar (ISAR) [9, 10, 11]. On the other hand, there are situations where the imaged scene is large scale. A representative example is the airborne synthetic aperture radar (SAR) imaging [12, 13]. In this case, the size of the sensing dictionary matrix may become prohibitive. Consequently, direct implementations of CS-based algorithms may become infeasible, if not impossible. This calls for the development of alternative approaches with a reduced complexity. In [14], ground-penetrating radar imaging is considered and the block-Toeplitz structure is used to dramatically reduce the size of the CS dictionary. As a result, it allows for a reduction in storage for each dimension. The dictionary used in [15] has this translational invariance in two dimensions and allows for the dictionary to be stored with more reduction in size.

In this paper, a new image formation approach is proposed, which combines the Fourier and sparsity-based reconstruction strategies. Herein, a Fourier-based reconstruction method is first applied to produce a coarse-resolution image. These images are then combined to produce a high-resolution image through the exploitation of sparse reconstruction techniques. The mapping between the coarse-resolution Fourier-based image and the fused high-resolution image in this stage allows the partition the entire image to multiple sub-images and process them separately. As such, the required complexity is significantly reduced as compared to the direct reconstruction of the entire image through CS-based techniques at the same time.

Notations: We use lower-case (upper-case) bold characters to denote vectors (matrices). $(.)^*$ implies complex conjugation, whereas $(.)^T$ denotes the transpose of a matrix or vector. $\|\cdot\|_2$ and $||\cdot||_1$ respectively denote the Euclidean (l_2) and l_1 norms.

2. SIGNAL MODEL

The signal model is presented in one-dimensional (1-D) range, but the proposed technique is applicable to two-dimensional (2-D) problems and simulation results will be presented for 2-D applications.

Consider a sparse scene with a size of N pixels and in the presence of K point targets, located at $x_1, \ldots, x_K$. Assume that a monostatic radar emits signal $s(t)$ to illuminate

the service area. The received signal can be expressed as

$$r(t) = \sum_{k=1}^{K} \sigma_k s\left(t - \frac{2x_k}{c}\right), \tag{1}$$

where σ_k is the corresponding reflectivity of the kth target and c is the propagation velocity.

3. IMAGING RECONSTRUCTION

In this section, we briefly summarize the two representative imaging reconstruction approaches which are respectively based on back-projection and CS.

3.1. Back-projection

The back-projection algorithm is implemented using a weighted matched filter with a hypothetic range x_i, i.e.,

$$\begin{aligned} g(x_i) &= \int w(t) r(t) s^*\left(t - \frac{2x_i}{c}\right) dt \\ &= \sum_{k=1}^{K} \sigma_k \rho\left(\frac{2(x_i - x_k)}{c}\right), \end{aligned} \tag{2}$$

for $1 \le i \le N$, where $w(t)$ is the window function and

$$\rho(\tau) = \int w(t) s(t) s^*(t-\tau) dt \tag{3}$$

is the point spread function (PSF).

To illustrate the problem, we depict examples of the PSF in Figs. 1(a) and 1(b) corresponding to rectangular and Blackman windows, where the transmit signal is a linear frequency modulated (LFM) signal with a bandwidth 20 MHz. The pixel size is set to 3 m. The Blackman window yields a much lower sidelobe level at the expense of a wider mainlobe. In Fig. 2, we show an example of a 1-D sparse scene together with the resulting back-projection images respectively using the two different PSFs. The sparse scene consists of $N = 200$ pixels with $K = 11$ targets, whose positions are identified using red lines. It is observed in Fig. 2(a) that most sparse signals are resolved with a high level of floor due to the sidelobe problem. In Fig. 2(b), on the other hand, the floor is reduced to a negligible level, whereas the waveform width is extended, making more targets unresolvable.

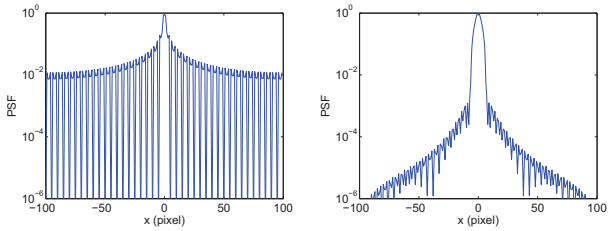

(a) Rectangle window (b) Blackman window

Fig. 1. PSF (K=11 and $N = 200$).

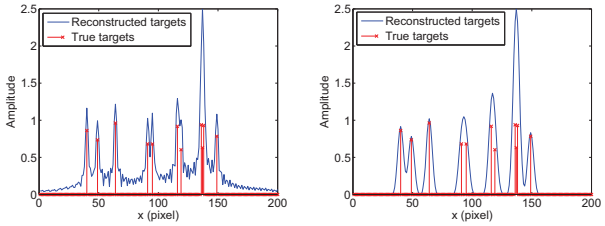

(a) Rectangle window (b) Blackman window

Fig. 2. Image reconstruction via matched filter (K=11).

3.2. Compressive Sensing Approach

The CS-based approach solves the inverse problem, depicted in Eq. (1), by finding the sparsest solution $\mathbf{q}$ from the following expression:

$$\mathbf{r} = \mathbf{B}\mathbf{q}, \tag{4}$$

where $\mathbf{r} = [r(t_1), ..., r(t_Q)]^T$ is a $Q \times 1$ vector that collects the observations at Q time intervals, $\mathbf{B} = [\mathbf{b}_1, ..., \mathbf{b}_N]$ is a sensing matrix whose kth column is expressed as

$$\mathbf{b}_k = \left[s\left(t_1 - \frac{2x_k}{c}\right), ..., s\left(t_Q - \frac{2x_k}{c}\right)\right]^T, \tag{5}$$

with $\mathbf{q} = [q_1, ..., q_N]^T$ being an $N \times 1$ vector to be determined. The indexes of the sparse entries in vector $\mathbf{q}$ represent the positions of the sparse targets, whereas their values represent the respective target reflectivities.

The above problem can be reformulated as the following constrained l_1-norm minimization problem

$$\hat{\mathbf{q}} = \arg\min_{\mathbf{q}} ||\mathbf{q}||_1 \quad \text{s.t.} \quad ||\mathbf{r} - \mathbf{B}\mathbf{q}||_2 < \epsilon, \tag{6}$$

where ϵ is a user-specific bound. This type of problem has been the objective of intensive studies in the area of CS, and a number of effective numerical computation methods have been developed. In this paper, we use the batch Lasso method, but other methods may also be used. Fig. 3 depicts the reconstructed image via the CS approach. As a comparison to back-projection, the CS approach results in a better resolution and it is clear that all the targets are identified.

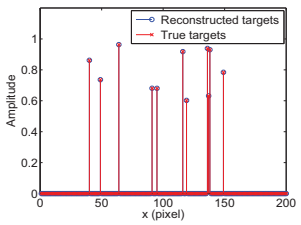

Fig. 3. Image reconstruction via Lasso (K=11).

4. PROPOSED RECONSTRUCTION APPROACH

As discussed earlier, conventional CS techniques demonstrate the capability of acquiring high-resolution images, such as aircrafts in ISAR, and human objects in ground-based TWRI. However, in very large-scale imaging applications, such as

airborne SAR imaging, the illuminated scene may extend to a large area, e.g., in the order of tens of kilometers. It thus becomes infeasible, if not impossible, to use conventional CS techniques for the reconstruction of such large-scale scenes due to the prohibitive computation and associated storage requirements.

In this section, we propose a novel segmented CS method by exploiting the characteristics of the PSF. Since the PSFs of transmitted waveforms have a finite support, as shown in Fig. 1, in the sense that there exists a value of η such that the value of $\rho(n)$, which is a discretized version of $\rho(\tau)$ described in terms of pixels, is negligible for $|n| > \eta$, i.e.,

$$\rho(n) \approx 0, \quad |n| > \eta. \tag{7}$$

This property is illustrated in Fig. 4. As such, it becomes feasible to segment the coarse image $\mathbf{g} = [g(x_1), ..., g(x_Q)]^T$ in Eq. (2) into multiple small sub-images. The CS-based imaging techniques are then applied at each segmented sub-image data to reconstruct high-resolution sub-scene images. As such, the sparse imaging problem is converted into a parallel set of imaging problems with much smaller sub-scenes which can be feasibly handled by conventional CS techniques.

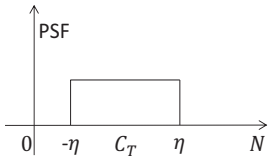

Fig. 4. PSF with a finite support.

Consider the vector-form expression of Eq. (2) as

$$\mathbf{g} = \mathbf{D}\mathbf{q}, \tag{8}$$

where the (i,k)th element of $\mathbf{D}$ is $\rho[2(x_i - x_k)/c]$ for $i = 1, \ldots, Q$ and $k = 1, \ldots, N$. Note that, because of Eq. (7), matrix $\mathbf{D}$ is a banded matrix with a finite support of $2\eta + 1$ elements. As such, the sparse reconstruction of vector $\mathbf{q}$ can be segmented into multiple parallel problems as detailed below.

The entire coarse image data $\mathbf{g}$ via back-projection is divided into M sub-images and the sub-image partition criterion is shown in Fig. 5. In each sub-image, we are interested in estimating $\mathbf{q}^{(m)} = [q(n_1^{(m)}), \ldots, q(n_2^{(m)})]$ with a width of $L = n_2 - n_1 + 1$ pixels. By considering the width of the PSF, the corresponding observation $\tilde{\mathbf{g}}^{(m)} = [g(n_1^{(m)} - \eta), \ldots, g(n_2^{(m)} + \eta)]$ includes all the data generated by the targets located within the imaging of interest region $\mathbf{q}^{(m)}$. However, due to the convoluting nature of the PSF, the observed data also include contributions from neighboring pixels, yielding inter-partition interference. Such interference is mitigated by reconstructing the sub-image over an extended region $\tilde{\mathbf{q}}^{(m)} = [q(n_1^{(m)} - 2\eta), \ldots, q(n_2^{(m)} + 2\eta)]$ as the region to be imaged because targets located outside of the $[n_1^{(m)} - 2\eta, n_2^{(m)} + 2\eta]$ region have negligible influence to the sub-image data in the area considered.

In practice, we may use a margin of ξ, which is suitably larger than η, to reduce the effect of sidelobes of the PSF. That is, $\check{\mathbf{g}}^{(m)} = [g(n_1^{(m)} - \xi), \ldots, g(n_2^{(m)} + \xi)]$ is used to image $\check{\mathbf{q}}^{(m)} = [q(n_1^{(m)} - 2\xi), \ldots, q(n_2^{(m)} + 2\xi)]$.

Based on the analysis above, we segment the entire coarse image $\mathbf{g}$ in Eq. (2) into M sub-images and acquire

$$\check{\mathbf{g}}^{(m)} = \mathbf{D}^{(m)}\check{\mathbf{q}}^{(m)}, \; m = 1, \ldots, M, \tag{9}$$

where $\mathbf{D}^{(m)}$ is the sensing matrix as the collection of $\mathbf{q}$ over a finite grid $[q(n_1^{(m)} - 2\xi), \ldots, q(n_2^{(m)} + 2\xi)]$.

Through the proposed segmentation approach, by exploiting the finite support of the PSF, the reconstruction of the entire scene can be divided into the multiple sub-scene reconstructions, and each sub-scene is recovered with a high resolution based on the CS technique. With respect to the sub-scene reconstruction in Eq. (9), the desired result of $\check{\mathbf{q}}^{(m)}$ is represented as the solution to the following constrained l_1-norm minimization problem

$$\hat{\mathbf{q}}^{(m)} = \arg\min_{\check{\mathbf{q}}^{(m)}} ||\check{\mathbf{q}}^{(m)}||_1 \tag{10}$$
$$\text{s.t.} \quad ||\check{\mathbf{g}}^{(m)} - \mathbf{D}^{(m)}\check{\mathbf{q}}^{(m)}||_2 < \epsilon^{(m)},$$

where $\epsilon^{(m)}$ is a user-specific bound. Note that the sparsity of the targets should satisfy the requirement in every sub-image, which is more strict than conventional CS approach as described in Section 3.2. Then, the interested region is obtained from $\hat{\mathbf{q}}^{(m)}$ as $\mathbf{q}^{(m)} = [\hat{q}^{(m)}(2\xi + 1), \ldots, \hat{q}^{(m)}(2\xi + L)]$.

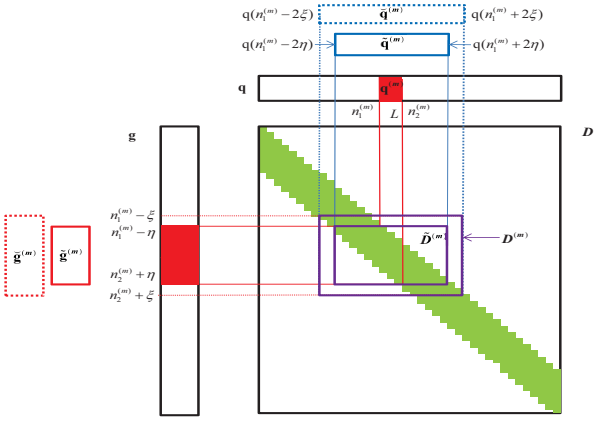

Fig. 5. Sub-image partition criterion.

5. SIMULATION RESULTS

We first present the results corresponding to the previous example depicted in Figs. 2 and 3. The number of pixels constructed in each partition is set to $L = 100$, yielding the number of sub-images to be $M = 2$. In addition, the Blackman window is exploited to reduce the sidelobe, whose support consists of $\eta \approx 8$ pixels and $\xi = 10$ is used. The results are presented in Fig. 6, which shows similar performance as in Fig. 3.

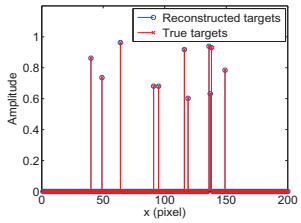

Fig. 6. Image reconstruction via proposed approach (K=11).

Next, as an example of large-scale problem, a 2-D scene, as depicted in Fig. 7(a), is considered, where $K = 500$ nonzero entries are randomly distributed in a region of 200×200 pixels. The 2-D PSF function, shown in Fig. 7(b), is assumed, which is the result of using the PSF depicted in Fig. 1(b) in both x- and y-axes. The yielding imaging based on back-projection is depicted in Fig. 7(c). For such a large scene, conventional CS techniques need high computation and storage requirements. In the proposed technique, the image is segmented into a set of sparse reconstruction problems with a smaller dimension, where an area of 60×60 pixels are used to reconstruct a sub-image of size 40×40, and the corresponding number of sub-images is $M = 25$. As such, the CS reconstruction can be implemented with a much smaller sensing matrix in each partition, and the proposed technique can handle a much larger scenario. Fig. 7(d) shows the reconstructed imaging using the proposed technique. Compared to back-projection, the proposed approach resolves all the targets with a fine resolution.

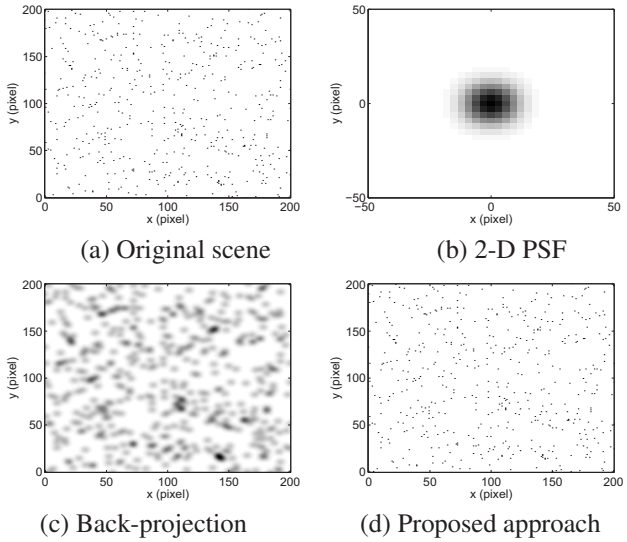

(a) Original scene (b) 2-D PSF

(c) Back-projection (d) Proposed approach

Fig. 7. Image reconstruction via proposed approach (K=500).

6. CONCLUSIONS

In this paper, we have proposed a compressive sensing algorithm that enables effective imaging process of a large-scale radar scene. The proposed technique utilizes the finite support property of the point spreading function and achieves high-resolution imaging with reduced computation complexity and storage requirements through image partitioning. The conditions for avoiding inter-partition interference were addressed, and the effectiveness of the proposed technique was verified by simulation results.

7. REFERENCES

[1] M. D. Desai and W. K. Jenkins, "Convolution backprojection image reconstruction for spotlight mode synthetic aperture radar," *IEEE Trans. Image Proc.*, vol. 1, no. 4, pp. 505-517, Oct. 1992.

[2] V. Krishnan, J. Swoboda, C. E. Yarman, and B. Yazici, "Multistatic synthetic aperture radar image formation," *IEEE Trans. Image Proc.*, vol. 19, no. 5, pp. 1290-1360, May 2010.

[3] Y. D. Zhang and A. Hunt, "Image and localization of behind-the-wall targets using linear and distributed apertures," in M. G. Amin (Ed.), *Through the Wall Radar Imaging*. CRC Press, 2010.

[4] B. D. Rigling, "Spotlight synthetic aperture rdar," in N. J. Willis and H. D. Griffiths (ed.), *Advances in Bistatic Radar*. SciTech, 2007.

[5] X. Mao, Y. D. Zhang, and M. G. Amin, "Two-stage Multi-static Passive SAR imaging with reduced complexity," in *Proc. IEEE Radar Conf.*, Cincinnati, OH, May 2014.

[6] X. Mao, Y. D. Zhang, and M. G. Amin, "Low-complexity sparse reconstruction for high-resolution multi-static passive SAR imaging," *EURASIP J. Advanced Sig. Proc.*, in press.

[7] D. L. Donoho, "Compressed sensing," *IEEE Trans. Inform. Theory*, vol. 52, no. 4, pp. 1289-1306, April 2006.

[8] Q. Wu Y. D. Zhang, M. G. Amin, and B. Himed, "Multi-static passive SAR imaging based on Bayesian compressive sensing," in *Proc. SPIE Compressive Sensing Conf.*, Baltimore, MD, May 2014.

[9] Q. Wu Y. D. Zhang, M. G. Amin, and F. Ahmad, "Through-the-wall radar imaging based on modified Bayesian compressive sensing," in *Proc. IEEE China Summit and Int. Conf. Signal and Inform. Proc.*, Xi'an, China, July 2014.

[10] M. G. Amin (ed.), *Compressive Sensing for Urban Radars*. CRC Press, 2014.

[11] L. Wang, L. Zhao, G. Bi, C. Wan, and L. Yang, "Enhanced ISAR imaging by exploiting the continuity of the target scene," *IEEE Trans. Geosci. Remote Sens.*, vol. 52, no. 9, pp. 5736–5750, Sept. 2014.

[12] X. Mao, D. Zhu, and Y. D. Zhang, "Knowledge-aided two-dimensional autofocus for synthetic aperture radar," in *Proc. IEEE Radar Conf.*, Ottawa, Canada, April–May 2013.

[13] M. Xing, Y. Wu, Y. D. Zhang, G. Sun, and Z. Bao, "Azimuth resampling processing for highly squinted synthetic aperture radar imaging with several modes," *IEEE Trans. Geosci. Remote Sens.*, vol. 53, no. 7, pp. 4339–4352, July 2014.

[14] K. Krueger, J. H. McClellan, and W. R. Scott, "3-D imaging for ground penetrating radar using compressive sensing with Block-Toeplitz structures," in *Proc. IEEE SAM Workshop*, June 2012.

[15] A. C. Gurbuz, J. H. McClellan, and W. R. Scott, "A compressive sensing data acquisition and imaging method for stepped frequency GPRs," *IEEE Trans. Signal Proc.*, vol. 57, no. 7, pp. 2640-2650, July 2009.